

ESR study of spin adducts of the direct electrocatalytic decomposition of light aliphatic alcohols in a polymer electrolyte fuel cell

M. K. Kadirov,^{a*} M. I. Valitov,^a I. R. Nizameev,^a D. M. Kadirov,^b and Sh. N. Mirkhanov^c

^aA. E. Arbuzov Institute of Organic and Physical Chemistry,
Kazan Research Center of the Russian Academy of Sciences,
8 ul. Akad. Arbuzova, 420088 Kazan, Russian Federation.
Fax: +7 (843 2) 73 2253. E-mail: kadirov2004@mail.ru

^bKazan State Technological University,
68 ul. Karla Markska, 420015 Kazan, Russian Federation

^cKazan State University,
8 ul. Kremlevskaya, 420008 Kazan, Russian Federation

Spin adducts of methanol and ethanol electrocatalytic oxidation were detected by the spin trap method using a tiny H₂/O₂ fuel cell (FC) designed for ESR *in situ* with a Nafion/Pt membrane electrode assembly. Spin adducts of intermediates of the direct electrooxidation of ethanol, which have not been observed earlier, were obtained by the variation of oxidation conditions, in particular, the FC potential. The work of the FC was controlled by monitoring the diagnostic curves potential—current density, power density—current density, and efficiency—power density.

Key words: fuel cell, polymer polyelectrolyte, diagnostic curves, methanol, ethanol, free radical, ESR spectroscopy, spin trap, spin adduct.

Increasing interest in the development of direct alcohol fuel cells (DAFC) with the proton-exchange membrane (PEM), especially working on methanol to put in action electric travel facilities, has recently been observed.¹ However, methanol has substantial drawbacks, for instance, it is relatively toxic, its boiling point is low (65 °C), and it is not primary fuel. Therefore, other alcohols, in particular, those obtained from biomasses, are considered as alternative types of fuels.

Ethanol is an attractive fuel for electric travel facilities based on fuel cells (FC), because it is not so toxic and is easily prepared by fermentation of sugar-containing raw materials. However, there are several unsolved problems, being a serious obstacle in practical use of DAFC.

1. High activation barrier of the direct electrochemical oxidation of alcohol (DEOA) at the anode.

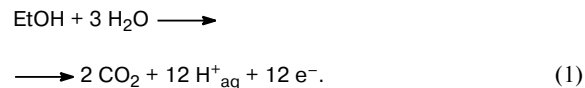
2. Contamination of the Pt catalyst with coproduct carbon monoxide (CO) formed during the DEOA. At present researchers try to solve these problems by using various, not purely platinum metallic catalysts, such as PdRu, PtRu, PtSnX (X = Ni, Co, Mn, V), which sometimes show a lower degree of contamination and better characteristics.^{2,3}

3. Penetration of an alcohol molecule through the polymer membrane.

4. Degradation of the proton-exchange membrane, because it works under rather extreme conditions: high working temperature (from 90 °C and higher), the action of metallic catalysis, and aggressive fuels and radical products of their decomposition, particularly, hydroxyl and superoxide radicals, *viz.*, HO[•] and HOO[•].

The use of ESR technique for detection of the radicals formed makes it possible to monitor and control reactions that occur on the surface and in the bulk of the PEM.

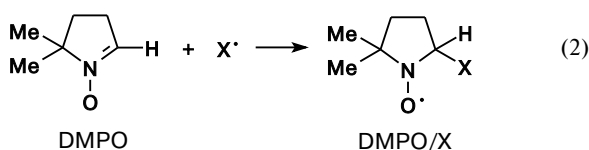
The complete oxidation of ethanol is a 12-electron process



Thus, many intermediates are involved in the reaction. Therefore, search for stage-by-stage investigation of this process is an urgent task.

A spin trap of the "nitrone" type, namely, 5,5-dimethyl-1-pyrroline-N-oxide (DMPO), was used to detect short-lived radicals in the working FC for ESR. The formation of the spin adduct DMPO/X from the DMPO spin trap and radical X[•] is given below (reaction (2)).

The spin adducts DMPO/X exhibit the characteristic ESR spectra with splittings from nitrogen and the proton



nearest the radical center. The large database on spin adducts are available at the site.⁴

Experimental

The ESR method was used to study processes and products in the FC.

By analogy to the prototype described earlier,⁵ we designed a FC for ESR more reliable and simpler in operation.⁶ The scheme of the FC for ESR is shown in Fig. 1.

The FC for ESR consists of body 1, cap 2, fluoroplastic tube 3, and membrane-electrode assembly 4. Channels providing access of hydrogen and oxygen and removal of their excess are made in the body and cap. Body 1 and cap 2 are connected in such a way that metallic tubes 5, which are the ends of two channels in the body, enter the corresponding two channels in the cap, and the channels are joined into a single system. The internal diameter of tube 3 is equal to the external diameter of the cylindrical FC mounted of two parts. The body and cap have holes for mounting of membrane-electrode assembly 4 consisting of the Nafion-type membrane with supported Pt particles

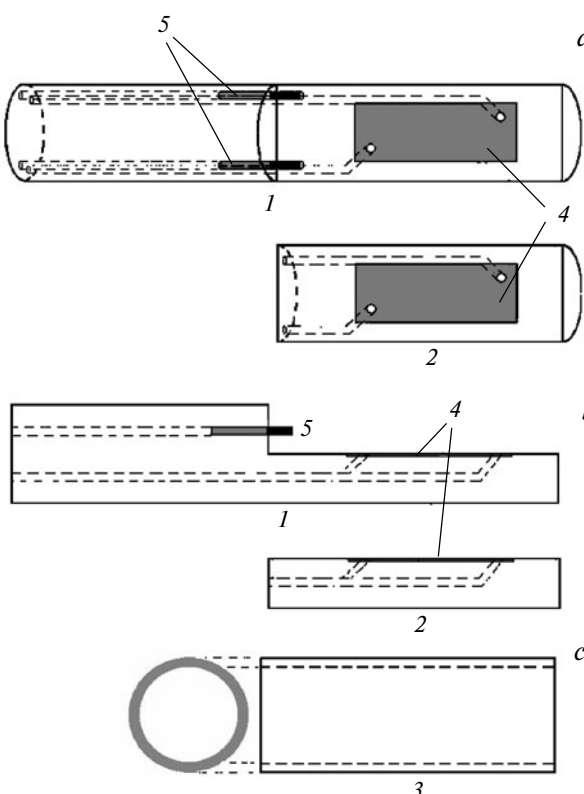


Fig. 1. Scheme of the fuel cell for ESR: *a*, front projection; *b*, sagittal projection; *c*, fluoroplastic tube. For clarification, see the text.

serving as the catalyst and grids of a thin Pt wire. The grids are arranged at two sides of the catalyst-covered membrane and serve as both electrodes and gas dividers.

First, fluoroplastic tube 3 is placed on a fluoroplastic cylinder, which is mounted of body 1 and cap 2 with membrane-electrode assembly 4 in the inner hole, thus transforming the components into a single whole. The electrodes are connected to the external circuit using thin silver connecting wires. Tubes, through which hydrogen and oxygen are fed to the FC under low pressure and their excess is removed, are connected to the channels. The side of the membrane-electrode assembly, where hydrogen comes through channels 1 and 2, serves as an anode, and the cathode is the side where oxygen comes. The FC is placed in the ESR spectrometer cavity in such a manner that the electric field lines of the cavity standing waves would be perpendicular to the surface covered with the catalyst of the membrane. Electrochemical reactions of hydrogen oxidation and oxygen reduction occur on the catalyst surface between the electrodes and membrane. Hydrogen atoms split into the component electron and proton on the catalyst surface in the negatively charged anodic part. Protons diffuse to the cathode through the membrane, and electrons move through the external circuit making useful work. The electrons reach the cathodic side and reduce oxygen atoms to bivalent ions. These ions form water and heat upon the reaction with diffused protons. The FC performs the direct conversion of the fuel energy to electricity, omitting poorly efficient combustion processes that occur with high losses.

Experiments were carried out with H_2/O_2 , *viz.*, FC for ESR with the surface density $0.2\text{--}1.0 \text{ mg cm}^{-2}$ Pt/Nafion 117. A 1 M solution of DMPO in water or alcohol ($10 \mu\text{L}$) was uniformly deposited on the anodic or cathodic side. Spectra were recorded 5 min after the beginning of the work of the FC under the short circuit conditions. Conventionally high potentials ($>0.3 \text{ V}$) were used, and low potentials ($<0.1 \text{ V}$) were also used in particular experiments, which is additionally mentioned during the description. The flow rate of hydrogen was $14 \text{ cm}^3 \text{ min}^{-1}$, and that of oxygen was $7 \text{ cm}^3 \text{ min}^{-1}$.

ESR spectra were detected on 3-cm EMX (Bruker), RadioPAN SE/X-2543, and RE-1306 radiospectrometers with frequencies of 9.3–9.9 GHz. The former two spectrometers are equipped with a rectangular cavity TE_{102} , and RE-1306 has a cylindrical cavity TM_{110} . The polarizing magnetic field was modulated with a frequency of 100 kHz, and the sensitivity of the spectrometers was $(1\text{--}5) \cdot 10^{12} \text{ spin T}^{-1}$. The polarizing magnetic field induction was measured with ER-035 and Sh1-1 NMR magnetometers and a Hall sensor. Frequencies in a microwave cavity were measured with an EiP371 frequency meter. The standard mode of ESR spectra detection was used with autotuning of the klystron signal frequency by the measuring cavity. The choice of detection modes was determined by requirements of undisturbed recording of the first derivative of the ESR signal. The measurement inaccuracy of magnetic parameters depends mainly on inaccuracies of the frequency meter and magnetometer, stability of resonance conditions, and ESR linewidth, being $\pm 3 \cdot 10^{-2} \text{ G}$ for HFC constants and $\pm 1 \cdot 10^{-4}$ for *g* factors.

Magnetoresonance parameters and relative intensities of spectral components were determined, as a rule, by computer simulation of experimental ESR spectra. The SimFonia (Bruker) and WinSim (NIEH/NIH) simulation programs were used, and the latter makes it possible to determine the basic parameters of the isotropic spectrum by automatic fitting.

Results and Discussion

The diagnostic curves (*I*) of the FC for ESR for the work with the H_2/O_2 fuel-oxidation system are shown in Fig. 2. The curve of the dependence of the power density on the current density shows (see Fig. 2, *a*) that the maximum current density of 34 mW cm^{-2} is achieved at a current density of 100 mA cm^{-2} . These values are more than an order of magnitude lower than the same characteristics of the known⁷ FC with the optimized parameters.

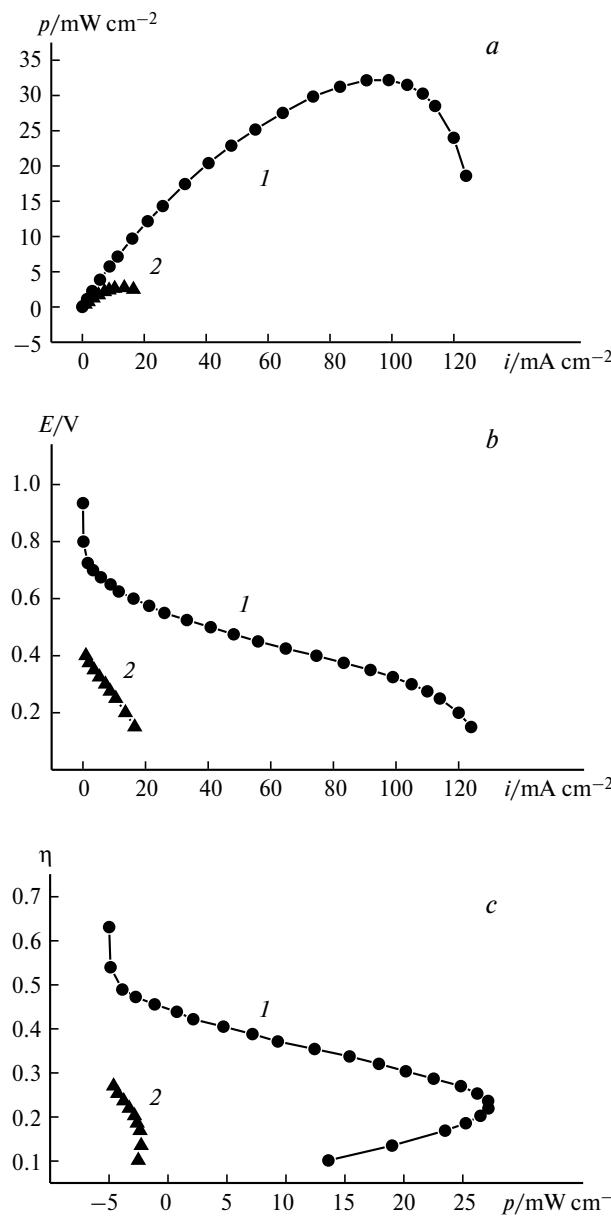


Fig. 2. Diagnostic curves of H_2/O_2 in the absence of (*I*) and with the addition (2) to the anodic side of $10 \mu\text{L}$ of an aqueous-ethanol (3 : 1) solution for the platinum–Nafion assembly with the surface density of Pt 1.0 mg cm^{-2} . For clarification, see the text.

The main reason for worsening of the characteristics is the absence of carbon support, which sharply increases the contact surface of platinum catalyst particles with the polyelectrolytic membrane. However, this fact does not impede to use the FC for ESR with the purpose of modeling processes in real low-temperature FC.

A comparison of the polarization curve (see Fig. 2, *b*) and the curve of the dependence of the power density on the current density (see Fig. 2, *a*) shows that the further increase in the current density after the power density maximum was achieved results in a decrease in the FC power because of the concentration polarization, which is caused by the depletion of the near-electrode space with reactants involved in the redox reactions.

Although the FC is not optimized to the maximum production of electric power, the efficiency of the input energy conversion to the useful energy is rather high, being $\sim 25\%$ (Fig. 2, *c*), which is due to the high efficiency of the method of electric energy generation in the FC.

The experimental spectrum (Fig. 3) of the DMPO spin adduct obtained on the anodic side of the FC for ESR is a triplet of triplets, where the small multiplet 1 : 1 : 1 is ascribed to one ^{14}N nucleus ($a_{\text{N}} = 16.2 \text{ G}$) and the large triplet 1 : 2 : 1 is ascribed to two equivalent

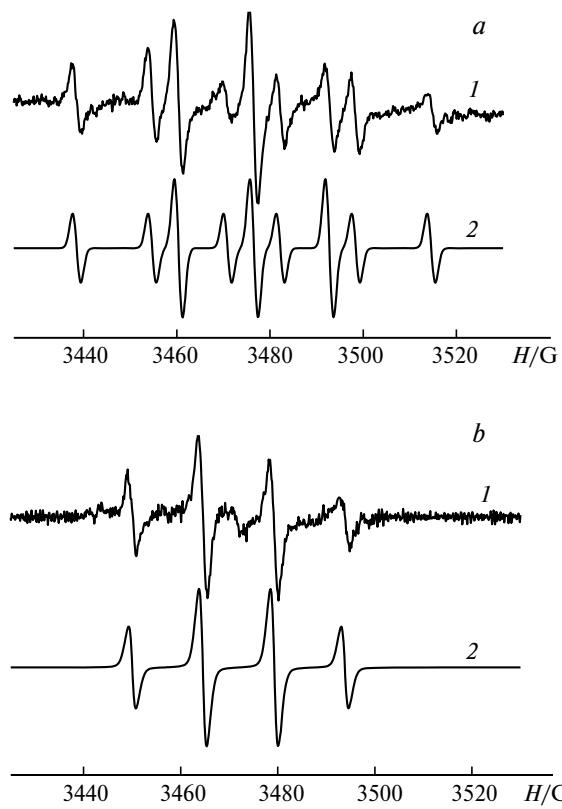
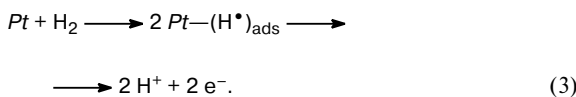


Fig. 3. Experimental ESR spectra of (*I*) spin adducts detected in an aqueous DMPO solution on the anodic (a) and cathodic (b) sides in the H_2/O_2 FC for ESR; (2) the corresponding simulated spectra.

^1H protons ($a_{\text{H}} = 21.8 \text{ G}$). The individual ESR linewidth is $\Delta H_{\text{pp}} = 2.0 \text{ G}$. The closest values of the constants met in literature are as follows: $a_{\text{N}} = 16.35 \text{ G}$, $a_{\text{H}} = 22.18 \text{ G}$ (see Ref. 8) and $a_{\text{N}} = 16.0 \text{ G}$, $a_{\text{H}} = 22.0 \text{ G}$ (see Ref. 9).

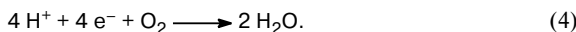
The spin adduct is formed in reaction (2), where $\text{X} = \text{H}$.¹⁰ Atomic hydrogen is generated from gaseous hydrogen on the catalyst surface during the oxidation of the fuel



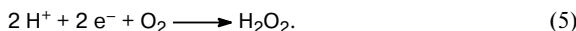
By definition, the potential of this reaction is $E_a^\circ = 0.000 \text{ V}$. In Eq. (3) the symbol of platinum is italicized to emphasize that the metallic surface is considered rather than one particular atom regardless of the mechanism of bonding with the hydrogen atom.

Under the same conditions, but with supporting of an aqueous DMPO solution on the cathodic side, the quartet ESR spectrum is observed for the spin adduct DMPO/OH (see Fig. 3, b) due to the same splitting from the ^{14}N nucleus ($a_{\text{N}} = 16.0 \text{ G}$) and ^1H proton ($a_{\text{H}} = 16.0 \text{ G}$). Here $\Delta H_{\text{pp}} = 1.7 \text{ G}$. The most similar published data are the following: $a_{\text{N}} = 14.7 \text{ G}$, $a_{\text{H}} = 14.7 \text{ G}$ (see Ref. 11) and $a_{\text{N}} = 14.8 \text{ G}$, $a_{\text{H}} = 14.8 \text{ G}$ (see Ref. 12).

The reactions at the cathode are the reduction of oxygen atoms by electrons coming from the anode through the electric circuit and addition of protons diffused from the anode through the membrane to form water with the equilibrium potential $E_c^\circ = 1.229 \text{ V}$



The DMPO/OH adduct is formed due to another reaction, which inevitably occurs at the cathode with the equilibrium potential $E_c^\circ = 0.682 \text{ V}$



Hydrogen peroxide decomposes instantly to two hydroxyl radicals on the surface of sponged platinum, which is really the platinum supported on Nafion. The results presented agree with the conclusions⁷ for the FC for ESR operated under the short circuit conditions.

Light aliphatic alcohols are actively studied as a potential fuel for FC. The deposition of $10 \mu\text{L}$ of a 1 M aqueous-methanol solution of DMPO on the anodic side of the FC for ESR and the work during more than 5 min under the short circuit conditions gave the experimental ESR spectrum (see Fig. 4, a). The decoding and automatic fitting of the spectrum indicate that we deal with the total spectrum of the adducts DMPO/CH₂OH (45%) and DMPO/H (55%). The origins of the hydrogen adduct was discussed above, and the DMPO/CH₂OH adduct

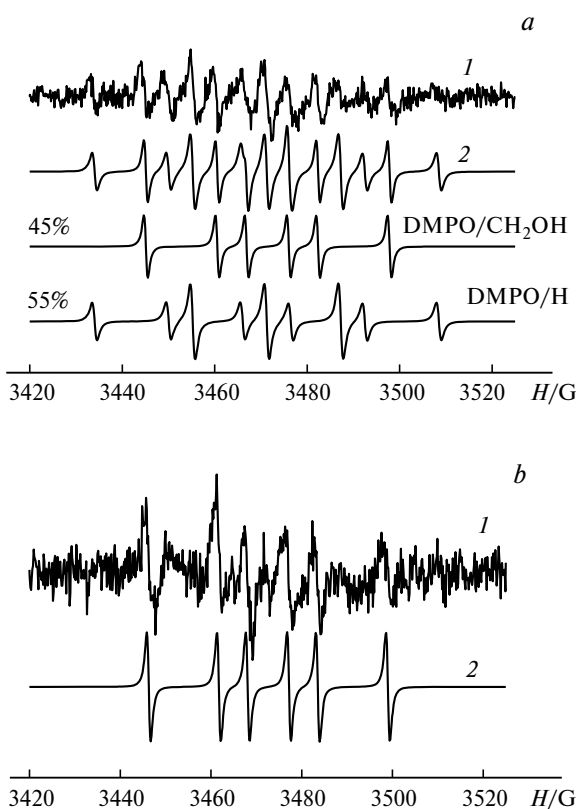


Fig. 4. Experimental ESR spectra of (1) spin adducts detected in an aqueous-methanol DMPO solution on the anodic (a) and cathodic (b) sides in the H_2/O_2 FS for ESR; (2) the total simulated spectra.

with the hyperfine coupling (HFC) constants $a_{\text{N}} = 15.4 \text{ G}$, $a_{\text{H}} = 21.8 \text{ G}$ is caused, most likely, by the direct anodic oxidation of methanol, and the $^{\bullet}\text{CH}_2\text{OH}$ radical is one of the primary radical products of this process. The literature data¹³ for this adduct are the following: $a_{\text{N}} = 15.92 \text{ G}$, $a_{\text{H}} = 22.56 \text{ G}$.

The weak spectrum of the same adduct DMPO/CH₂OH is detected when depositing an aqueous-methanol solution of DMPO on the cathodic side (see Fig. 4, b). The free radical $^{\bullet}\text{CH}_2\text{OH}$ is the result of the attack of the methanol molecule by the hydroxyl radical. However, no spin adduct of the hydroxyl radical itself was observed under these experimental conditions.

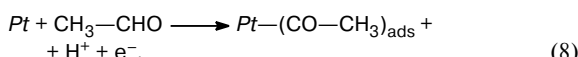
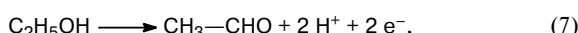
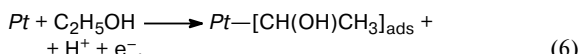
The diagnostic curves (2) of the H_2/O_2 FC for ESR with the membrane-electrode assembly 1 mg cm^{-2} Pt/Nafion obtained by the addition of $10 \mu\text{L}$ of an aqueous-ethanol (3 : 1) solution to the anodic side are also presented in Fig. 2. As can be seen from the polarization curve, the potential and current density values decrease sharply and, hence, the power density decreases (more than tenfold). The efficiency η also decreases, being 15%, while for the pure H_2/O_2 FC it is 25. This worsening of the FC characteristics is related, first of all, to the contamination of the Pt catalyst with coproduct carbon

monoxide (CO) formed during the DAFC, which is the main obstacle in the application of alcohols as fuel for FC.

As shown by IR spectroscopy,^{14–17} pure Pt electrodes are rapidly poisoned with such strongly adsorbed intermediates as CO due to dissociative chemisorption, which is the main reason for worsening of the FC characteristics. Other compounds were also identified by IR spectroscopy: reaction intermediates, such as acetaldehyde, and acetic acid, and other by-products.¹⁶ Using α -(4-pyridyl-1-oxide)-*N*-*tert*-butylnitrone (POBN) as a spin trap and the hydrogen/oxygen FC for ESR in an aqueous-ethanol solution, we detected the spin adduct POBN/CH(OH)CH₃ on the cathodic side, whereas the spin adducts POBN/CH(OH)CH₃ and POBN/H were observed on the anodic side.¹¹ The appearance of the $^{\bullet}\text{CH}(\text{OH})\text{CH}_3$ radical on the cathodic side was explained by the attack of ethanol molecules by the hydroxyl radicals, whereas their formation on the anodic side is due to the partial electrochemical oxidative decomposition of an alcohol molecule.

The use of DMPO as a spin trap made it possible to obtain additional information. For example, the adduct DMPO/OH ($a_N = 14.1$ G, $a_H = 14.1$ G, similar literature data²⁰: $a_N = 14.3$ G, $a_H = 14.3$ G) is formed along with the spin adduct DMPO/CH(OH)CH₃ ($a_N = 15.5$ G, $a_H = 22.2$ G, literature data: $a_N = 15.5$ G, $a_H = 22.2$ G;¹⁸ $a_N = 15.7$ G, $a_H = 22.4$ G (see Ref. 19) in the ratio 1 : 4 on the cathodic side (Fig. 5, a). The spin adducts DMPO/CH(OH)CH₃ and DMPO/H were observed on the anodic side (see Fig. 5, b), indicating, as published earlier,¹² the partial electrochemical oxidative of an ethanol molecule and splitting of a hydrogen molecule on the platinum surface to atoms.

The work of the FC at low potentials found the spin adducts DMPO/CH(OH)CH₃ ($a_N = 15.7$ G, $a_H = 23.0$ G) and DMPO/COCH₃ ($a_N = 14.9$ G, $a_H = 18.8$ G, literature data²¹: $a_N = 13.3$ G, $a_H = 17.5$ G) on the anodic side of the FC (see Fig. 5, c), indicating that the following reactions occur:



In addition, the spin adduct DMPO/OH ($a_N = 14.6$ G, $a_H = 14.5$ G) was detected, which is the result, most likely, of the dissociative adsorption of water



Thus, the ESR detection of the spin adducts of electrocatalytic ethanol oxidation *in situ* in the FC allowed us to record the polarization curves and spectra

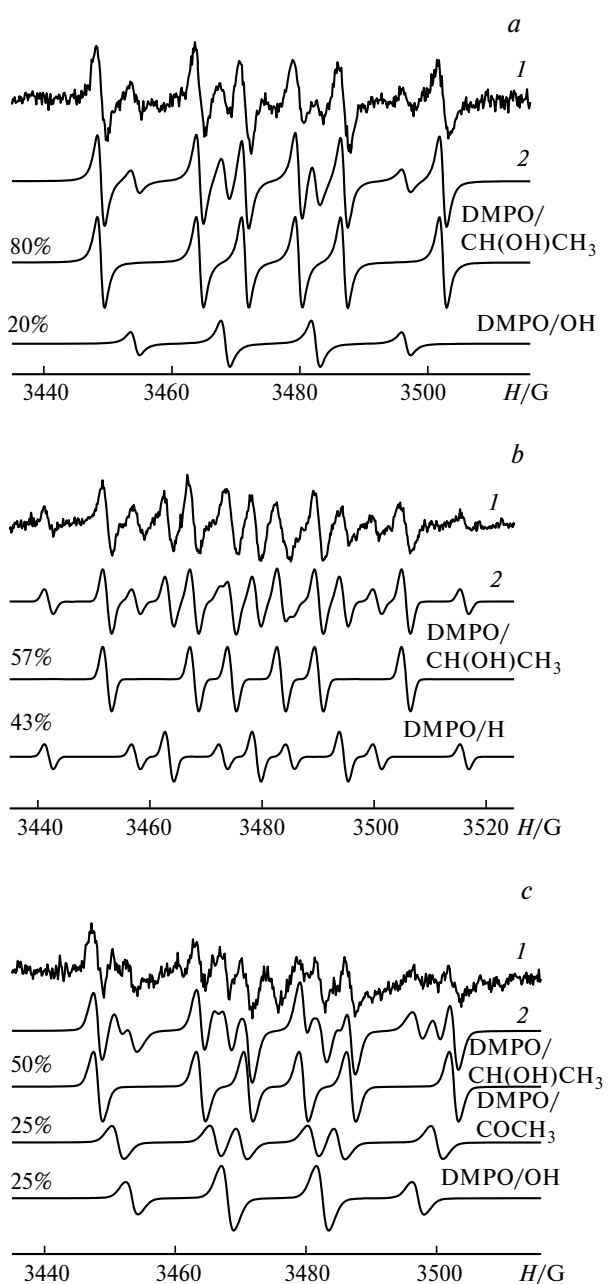


Fig. 5. Experimental ESR spectra of (1) spin adducts detected in an aqueous-ethanol DMPO solution on the cathodic (a), anodic (b), and anodic at low potentials (c) sides in the H₂/O₂ FC for ESR; (2) the total simulated spectra.

of the spin adducts. The paramagnetic intermediates of ethanol electrooxidation were specified by the variation of the FC potential.

This work was financially supported by the Russian Foundation for Basic Research (Project No. 09-03-12264-ofi-m), the Presidium of the Russian Academy of Sciences (Program for Basic Research No. 18), and the State Contract No. 02.352.11.7070.

References

1. C. Lamy, J.-M. Leger, S. Srivinasan, in *Modern Aspects of Electrochemistry*, Ed. J. O'M. Bockris, Plenum, New York, 2001, Vol. **34**, Ch. 3, p. 68.
2. M. R. Tarsevich, A. V. Kuzov, A. L. Klyuev, V. N. Titova, *Al'ternativnaya energetika i ekologiya [Alternative Energetics and Ecology]*, 2007, **46**, No. 2, 113 (in Russian).
3. A. Yu. Tsivadze, M. R. Tarsevich, V. N. Andreev, V. A. Bogdanovskaya, B. N. Efremov, N. A. Kapustina, V. N. Titova, A. A. Yavich, N. N. Belova, P. V. Mazin, *Al'ternativnaya energetika i ekologiya [Alternative Power Engineering and Ecology]*, 2007, **48**, No. 4, 57 (in Russian).
4. <http://epr.niehs.nih.gov>
5. A. Panchenko, H. Dilger, E. Möller, T. Sixt, E. Roduner, *J. Pow. Sources*, 2004, **127**, 320.
6. Pat. RF 66 540; *Byull. Izobret. [Invention Bulletin]*, 2007, No. 25 (in Russian).
7. M. Danilczuk, F. D. Coms, Sh. Schlick, *J. Phys. Chem.*, 2009, **113**, 8031.
8. F. Laurencelle, R. Chahine, J. Hamelin, K. Agbossou, M. Fournier, T. K. Bose, A. Laperriere, *Fuel Cells*, 2001, **1**, 66.
9. R. Hedrick, M. D. Webb, J. D. Zimbrick, *J. Radiat. Biol.*, 1982, **45**, 435.
10. A. Panchenco, Ph. D. Dissertation, Stuttgart, 2004, p. 154.
11. N. Motohashi, I. Mori, *J. Inorg. Biochem.*, 1986, **26**, 205.
12. A. Panchenko, H. Dilger, J. Kerres, M. Heir, A. Ullrich, T. Kaz, E. Roduner, *Phys. Chem. Chem. Phys.*, 2004, **6**, 2891.
13. D. L. Haire, P. H. Krygsman, E. G. Janzen, U. M. Oehler, *J. Org. Chem.*, 1988, **53**, 4535.
14. J. V. Perez, B. Beden, F. Hahn, A. Aldaz, C. Lanus, *J. Electroanal. Chem.*, 1989, **262**, 251.
15. T. Iwasita, E. Pastor, *Electrochim. Acta*, 1994, **39**, 531.
16. H. Hitmi, E. M. Belgsir, J.-M. Leger, *Electrochim. Acta*, 1994, **39**, 407.
17. B. Beden, J.-M. Leger, C. Lamy, in *Modern Aspects of Electrochemistry*, Eds J. O'M. Bockris, B. E. Conway, R. E. White, Plenum, New York, 1992, **22**, Ch. 2, p. 97.
18. A. Bosnjakovic, Sh. Schlick, *J. Phys. Chem.*, 2006, **110**, 10720.
19. A. J. F. Searle, A. Tomasi, *J. Inorg. Biochem.*, 1982, **17**, 161.
20. K. Makino, H. Imaishi, S. Marinichi, *Biochem. Biophys. Res. Commun.*, 1986, **141**, 381.
21. S. P. Yarkov, V. N. Voevodskii, V. E. Zubarev, *Khim. Vys. Energ.*, 1980, **14**, 115 [*High Energy Chem. (Engl. Transl.)*, 1980, **14**, No. 2].

*Received February 19, 2010;
in revised form June 1, 2010*